Theoretical study on stereodynamics of H + NeH$^+$ (*v*=0, *j*=0) → NeH$^+$ +H reaction

Zhenhua Gao, Meishan Wang*and Zhen Wang

School of Physics and Optoelectronics Engineering, Ludong University, Yantai 264025, China

Abstract. The stereodynamics of reaction H + NeH$^+$ (*v*=0, *j*=0) → H + NeH$^+$ is studied on a new potential energy surface (PES) constructed by Lü *et al.*, using the quasi-classical trajectory (QCT) method. The influence of collision energy for the reaction H + NeH$^+$ (*v*=0, *j*=0) → H + NeH$^+$ has been studied. The distributions of $P(\theta_r)$, $P(\phi_r)$ and PDDCSs have been calculated at four different collision energies. It can be found that the product rotational angular momentum j' aligned along the y-axis. Moreover, the product rotational angular momentum vector j' is preferentially oriented along the positive direction of y-axis at low collision energy, but preferentially oriented along the negative direction of y-axis at high collision energy. The results indicate the collision energy plays an important part in the stereodynamics of the title reaction.

1 Introduction

In order to understand those interesting phenomenons that include the interstellar processes, planetary ionospheres, and electric discharges, the ion-molecules reactions containing rare gas atoms are very necessary to investigate. Therefore, the proton scattering of rare gas atoms had offered a good research object in the past decades. In 1993, Pendergast *et al.* [1] employed the coupled-electron method to establish an accurate potential energy surface (PHHJ3) of the ground state of the NeH$_2^+$ system. Shortly after, the state-to-state reaction probabilities were reported by Kress *et al.* [2] with an approximate quantum dynamics calculation. Gilibert and co-workers [3-4] applied the coupled-states approximation to calculate the state selected integral cross sections as a function of collision

energy. In 2008, Mayneris *et al.* [5] calculated the reaction probabilities and cross sections of the $Ne + H_2^+/Ne + HD^+/Ne + HT^+$ in a wide range of collision energy by using a time dependent real packet quantum method on the PHHJ3 PES. In order to study the influence of vibrational excitation, Mayneris-Perxachs *et al.* [6] applied the time-dependent quantum dynamics method at the centrifugal sudden level (CS-RWP method) to study the reaction probabilities and cross sections of the $Ne + H_2^+$ (*v*=0-9, *j*=0) and D_2^+ (*v*=0-12, *j*=0) proton transfer reactions. In 2010, Lü *et al.* [7] constructed the ground state ($1^2A'$) analytical potential energy surface (LZHH PES) that was fitted using 7000 energy points. Based on the LZHH PES, some theoretical researches about the reaction $Ne + H_2^+ \rightarrow H_2^+ + Ne$ have been done. In 2011, Xiao *et al.* [8-10] investigated the isotopic effects and influences of the collision energies to vector correlations between reagents and products by using quasi-classical trajectory (QCT) method. Wang *et al.* [11] investigated dynamics of $Ne + H_2^+$ by QCT method, which reagent molecules are in different collision energy or vibrational States. The results showed that the reagent vibrational excitation had greater influence on the polarization of the product rotational angular momentum vectors j' than the collision energy. Ge *et al.* [12] calculated the dynamics of the $Ne+H_2^+$ using QCT method, which indicated that the reaction is dominated by forward-scattering and the NeH^+ product showed rotationally hot and vibrationally cold distributions. The product polarizations in the reactions $H + NeH^+/NeD^+/NeT^+ \rightarrow H_2^+/HD^+/HT^+ + Ne$ were studied by Zou *et al.* [13] using the QCT method. Moreover, the effects of the potential well on stereodynamics of the above reactions were discussed in their work. Yin *et al.* [14, 15] investigated the effects of collision energy, vibrational and rotational excitation of reagent molecules on the dynamic of the $H + NeH^+$ by QCT method. The results demonstrated that the title reaction was a typical barrierless atom (ion)–ion (molecule) reaction and was mainly dominated by the direct reaction mechanism.

From the above, most of the studies have focused on the reaction $Ne + H_2^+$, its reverse reaction $H + NeH^+$ and those isotopic effects. However, the exchange reaction $H + NeH^+ \rightarrow NeH^+ + H$ has seldom been studied to date. We will adopt a QCT calculation on the new LZHH PES in this paper to shed more light on this exchange reaction.

2 Theory

The standard quasiclassical trajectory (QCT) method is employed to investigate the stereodynamics of the title reaction in this paper. Details of the QCT method can be found in Refs [19-22], and only the most important details are described here.

2.1 QCT calculation

The classical Hamilton's equations are integrated in three dimensions numerically. Four collision energies (20, 40, 60, 80 kcal/mol) were chosen for the title reaction. The rotational and vibrational levels of NeH^+ were taken as *j*=0 and *v*=0, respectively. Batches of

100000 trajectories were calculated for each reaction and the integration step size is chosen as 0.1 fs in this calculation. The trajectories were started at an initial distance of 15Å between the H atom and the centre of the most of the NeH^+ molecule. In the QCT framework, for selected collision energy (E_t) and the given rovibrational state (v,j) of LiH, the reaction cross section $\sigma_r(E_t,v,j)$ can be written as:

$$\sigma_r = \pi b_{max}^2 \lim \frac{N_r}{N_t}. \tag{1}$$

Where b_{max} denotes the maximum value of the reactive impact parameter for the collision energy.

Fig. 1 illustrates the CM reference frame used in the present investigation. The k and k' are the reactant relative velocity and product relative velocity respectively. k is parallel to the z-axis, and y-axis is perpendicular to the x-z plane containing k and k' vectors. The final product angular momentum is j', with its polar and azimuthal angles being θ_r and ϕ_r respectively. The θ_t between k and k' is defined as the scattering angle.
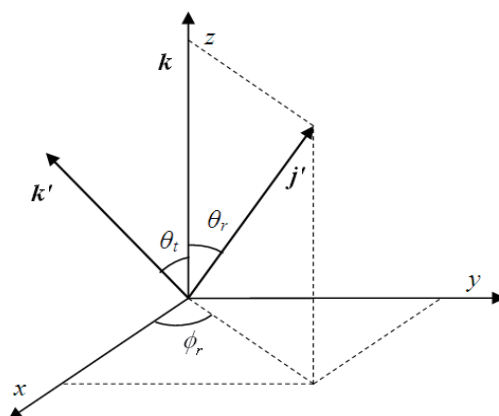

Figure 1: The center-of-mass frame used to describe the k, k' and j' correlations.

The distribution function $P(\theta_r)$ describes the k-j' correlation and can be expanded in a series of Legendre polynomials as:

$$P(\theta_r) = \frac{1}{2}\sum[2k+1]a_0^{(k)}P_k(\cos\theta_r). \tag{2}$$

The expanding coefficients $a_0^{(k)}$ called polarization parameters are given by

$$a_0^{(k)} = \int_0^\pi P(\theta_r)P_k(\cos\theta_r)\sin\theta_r d\theta_r = \langle P_k(\cos\theta_r)\rangle. \tag{3}$$

The coefficients $a_0^{(k)}$ are called orientation parameter (when k is odd) or alignment parameter (when k is even). As $k=2$, the expression for the expansion coefficient $a_0^{(2)}$ is

written as,

$$a_0^{(2)} = \langle P_2(\cos\theta_r)\rangle = \langle P_2(j\cdot k)\rangle = \frac{1}{2}\langle 3\cos^2\theta_r - 1\rangle. \tag{4}$$

The dihedral angle distribution function $P(\phi_r)$ representing the k-k'-j' vector correlation can be expanded in a series of Fourier as [38,40]

$$P(\phi_r) = \frac{1}{2\pi}\left(1 + \sum_{even,n\geq 2} a_n\cos n\phi_r + \sum_{odd,n\geq 1} a_n b_n\sin n\phi_r\right) \tag{5}$$

with

$$a_n = 2\langle\cos n\phi_r\rangle \quad \text{and} \quad b_n = 2\langle\sin n\phi_r\rangle.$$

In this paper, $P(\phi_r)$ is expanded up to n = 24, which shows good convergence. The PDDCSs can be represented as follows:

$$P(\omega_t,\omega_r) = \sum_{kq}\frac{[k]}{4\pi}\frac{1}{\sigma}\frac{d\sigma_{kq}}{d\omega_t}C_{kq}(\theta_r,\phi_r)^*. \tag{6}$$

Where $[k]=2k+1$, $C_{kq}(\theta_r,\phi_r)$ refers to the modified spherical harmonics. k denotes the quantum number of the product rotational angular momentum and q denotes the magnetic quantum number of the product rotational angular momentum. $\frac{1}{\sigma}\frac{d\sigma_{kq}}{d\omega_t}$ is a generalized PDDCS, and $\frac{1}{\sigma}\frac{d\sigma_{kq}}{d\omega_t}$ yields

$$\frac{1}{\sigma}\frac{d\sigma_{k0}}{d\omega_t} = 0, \qquad\qquad k \text{ is odd} \tag{7}$$

$$\frac{1}{\sigma}\frac{d\sigma_{kq+}}{d\omega_t} = \frac{1}{\sigma}\frac{d\sigma_{kq}}{d\omega_t} + \frac{1}{\sigma}\frac{d\sigma_{k-q}}{d\omega_t} = 0, \quad k \text{ is even and } q \text{ is odd, or } k \text{ is odd and } q \text{ is even} \tag{8}$$

$$\frac{1}{\sigma}\frac{d\sigma_{kq-}}{d\omega_t} = \frac{1}{\sigma}\frac{d\sigma_{kq}}{d\omega_t} - \frac{1}{\sigma}\frac{d\sigma_{k-q}}{d\omega_t} = 0, \quad k \text{ and } q \text{ are even, or } k \text{ and } q \text{ are odd.} \tag{9}$$

In Eqs. (8) and (9), the symbol $\pm$ in $\frac{1}{\sigma}\frac{d\sigma_{kq\pm}}{d\omega_t}$ represent the sum or difference between $\frac{1}{\sigma}\frac{d\sigma_{kq}}{d\omega_t}$ and $\frac{1}{\sigma}\frac{d\sigma_{k-q}}{d\omega_t}$.

$(2\pi/\sigma)(d\sigma_{00}/d\omega_t)$, $(2\pi/\sigma)(d\sigma_{20}/d\omega_t)$, $(2\pi/\sigma)(d\sigma_{22+}/d\omega_t)$, and $(2\pi/\sigma)(d\sigma_{21-}/d\omega_t)$ are calculated in this paper.

2.2 The theoretical basis of constructing the PES

In the present calculations, we use the new 3D adiabatic PES constructed by Lü *et al.* The PES was developed by fitting the energy points that were calculated by using the complete active space self-consistent field and internally contracted multireference configuration interaction. In both CASSCF and MRCI calculations, ten active orbital included nine valence electrons (8a'+2a''), consisting of H 1s orbital and the 2s, 2p, 3s and 3p orbital

of the Ne atom. The remaining orbital was kept doubly occupied. Equal weights were assigned to each of the three states (12A', 22A'', 12A'') in the state-averaging calculations. Moreover, the multireference Davison correction [16] (+Q) was included to compensate for the effect of higher order correlation. The analytical representation of the PES was fitted with 7026 *ab initio* energies below 2.8 eV relatived to the dissociation energy of Ne + H_2^+. The analytical expression of the PES was showed by the Aguado-Paniagua function [17]. The root mean square error was 0.27kcal/mol and the maximum energy deviation was 2.7kcal/mol, which is more accurate than previous PES [1]. The cross sections (v=0, j=1) taken into consideration the Coriolis coupling effect based on the new PES are found to be in perfect agreement with the available experimental data [18]. Only a deep well at the collinear allocation on the LZHH PES, and no other barriers orwells were found on this PES. The depth of well becomes shallower and a barrier appears with the decrease of Ne-H-H angle.

3   Results and discussion

3.1   Scalar properties of reaction

The integral cross sections of the H + NeH$^+$ (v=0, j=0) $\rightarrow$ H + NeH$^+$ reaction with the increasing of collision energy are calculated and discussed.

As shown in Fig. 2, the results show the decreasing tendency of integral cross section when the collision energy increase from 5 to 20 kcal/mol (low collision energy) but the increasing tendency of integral cross section when the collision energy increase over the range of 20-80 kcal/mol (high collision energy). The reason for this interesting phe-
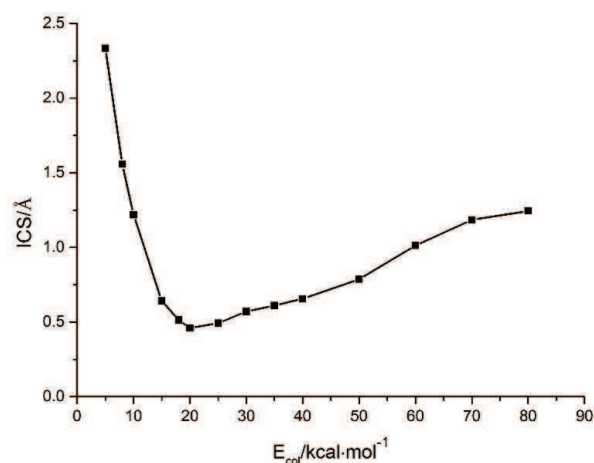

Figure 2: Integral cross section of the H + NeH$^+$ (v=0, j=0) $\rightarrow$ H + NeH$^+$ reaction as a function of collition energy.

nomenon is that title reaction mainly governed by the potential well at low collision energy, but the potential barrier play an important role when the collision energies are high.

3.2   Vector properties of reaction dynamics

To get a better graphical representation of the polarization of the products NeH^+, we have plotted the diagram of $P(\theta_r)$ and $P(\phi_r)$ which describe the spatial distribution of the product rotational angular momentum vector j' at four different collision energies in Figs. 3 and 5 respectively.
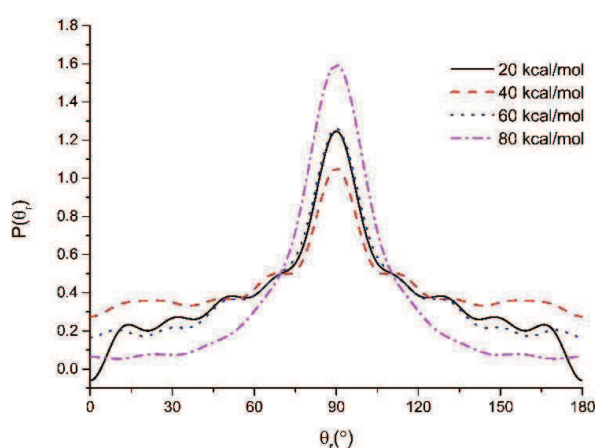

Figure 3: Angular distribution of $P(\theta_r)$, reflecting the k-j' correlation, at E_{col}= 20, 40, 60 and 80 kcal/mol.

The $P(\theta_r)$ distribution of j' describes the k-j' correlation. From Fig. 3, one can find that the peaks of the $P(\theta_r)$ distribution appear at θ_r angles close to $90°$ and the $P(\theta_r)$ distributions are symmetric with respect to $90°$. It demonstrates that the product rotational angular momentum vector j' is distributed with cylindrical symmetry in the product scattering frame, and the direction of j' is preferentially aligned perpendicular to the direction of k. The peak of $P(\theta_r)$ becomes narrower and lower with the increase of the collision energy from 5 to 20 kcal/mol, which denotes that the product rotational alignment becomes weaker with the collision energy increase. However, the peak of $P(\theta_r)$ becomes broader and higher as the collision energy increases to 80 kcal/mol, which means that the degree of rotational alignment of the product has an increasing trend when the collision energies continue to increase. In order to obtain a better understanding of the alignment degree of the product, we calculate the product alignment parameter $\langle P_2(j' \cdot k)\rangle$, which are shown in Fig. 4.

This variation tendency of $\langle P_2(j' \cdot k)\rangle$ is consistent with the variation trend of $P(\theta_r)$. The smaller the value of $\langle P_2(j' \cdot k)\rangle$ is, the stronger the alignment of product is. From the Fig. 4, one can know that the values of the product average rotational alignment parameter $\langle P_2(j' \cdot k)\rangle$ confirmed this trend. According to the report by Han *et al.* [23], the
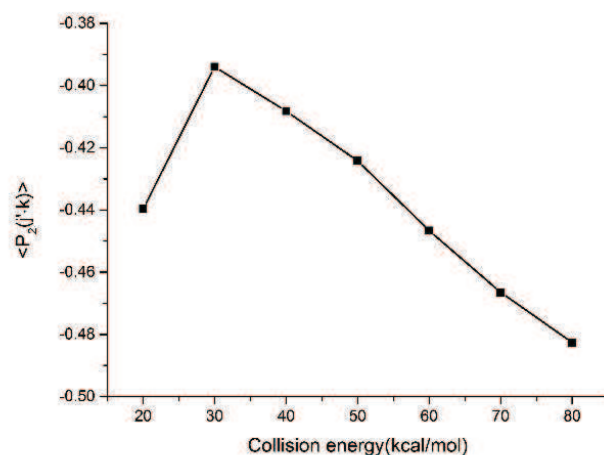
Figure 4: Product rotational alignment parameter $\langle P_2(j'\cdot k)\rangle$ as a function of collision energy.

rotational alignments of products are sensitive to two main factors: one is the charac-ters of the PES, and the other is the mass factor. The tendency of $\langle P_2(j'\cdot k)\rangle$ for the title reactions is in accordance with attractive PES, which means that the exoergic process of the title reaction occurs on the entrance valley of the PES. The decrease of the degree of product rotational alignment with the increase of collision energy from 20 to 40 kcal/mol is result in the well on the PES. When the collision energy becomes lower, some trajecto-ries will be "trapped" in the well. The existence of potential well on PES lead complex to have longer lifetime, which cause angular momentum lose memory of initial direction [24, 25]. As a result, the product rotational polarization becomes weak at low collision energies. Even so, when the collision energy is high enough, the product NeH^+ with higher internal energy can move with less effort away from the potential well. Therefore, the degree of product alignment indicates perfect augment with the increase of collision energy.

The dihedral angle distribution of $P(\phi_r)$ that describes the k-k'-j' correlation is shown in Fig. 5. From Fig. 5, one can find that the $P(\phi_r)$ distributions are asymmetric with respect to the k-k' scattering plane (or about ϕ_r=180°), which directly reflects the strong polarization of product rotational angular momentum. The peaks of $P(\phi_r)$ appear at ϕ_r=90° and 270°, which indicates that the rotational angular momentum vector of prod-uct NeH^+ is aligned along y-axis of CM frame. As the peak at ϕ_r= 90° is not equal to that at ϕ_r=270° for a fixed collision energy, the product rotational angular momentum vector j' is not only aligned, but also oriented along the y-axis. The peak at ϕ_r=90° is higher than that at ϕ_r=270° at 20 kcal/mol collision energies, which indicates the j' is preferentially oriented along the positive direction of y-axis. While the peak at ϕ_r=90° is lower than that at ϕ_r=270° over 40-80 kcal/mol collision energies, which indicates the j' is preferentially oriented along the negative direction of y-axis. The distribution of $P(\theta_r)$ is symmetric, while the distribution of $P(\phi_r)$ is asymmetrical. The reason may be the repulsive energy
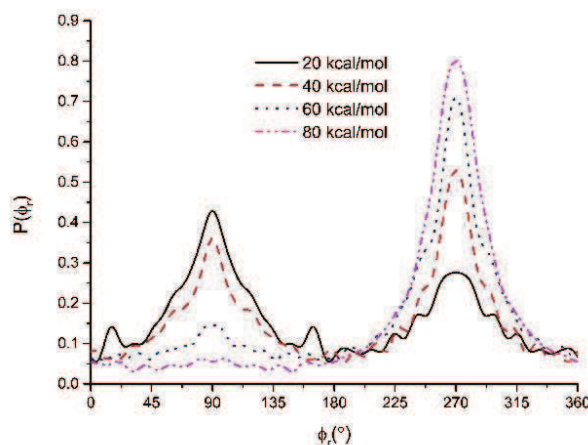
Figure 5: Dihedral angle distribution of j', $P(\phi_r)$, with respect to the k-k' plane, for product NeH$^+$ from H + NeH$^+$ (v=0, j=0) $\rightarrow$ H + NeH$^+$ at E_{col} = 20, 40, 60 and 80 kcal/mol.

between Ne-H$^+$ atoms, leading to the violation of the symmetry when the reaction takes place. The "Impulsive-Collision Model" [26, 27] of the atom-molecule reaction developed by Han *et al.* can explain the behavior. In reaction A + BC $\rightarrow$ AB + C, the product rotational angular momentum j' can be compiled as:

$$j' = L\sin^2\beta + j\cos^2\beta + J_1 m_B / m_{AB} \tag{10}$$

$$\cos^2\beta = \frac{m_A m_C}{(m_A + m_B)(m_B + m_C)} \tag{11}$$

$$J_1 = \sqrt{\mu_{BC} E_c} (\vec{r}_{AB} \times \vec{r}_{CB}) \tag{12}$$

where L and j are the orbital and rotational angular momentum of the reactant molecule AB, respectively. $\vec{r}_{AB}$ and $\vec{r}_{CB}$ is unit vectors where B pointing to A and C, respectively. The reduced mass of the BC molecule is represented by the μ_{BC} and E_c is the repulsive energy between B and C atoms. The term $L\sin^2\beta + j\cos^2\beta$ in the equation is symmetric with respect to the k-k' scattering plane, however, the term $J_1 m_B / m_{AB}$ has a preferred direction because of the effect of the repulsive energy, which gives rise to the orientation of the products NeH$^+$ during the chemical bond forming and breaking for the title reaction.

As is shown in Fig. 6, the scattering direction of the product molecule and the k-k'-j' correlation are described by the generalized polarization-dependent differential cross sections (PDDCSs). The PDDCS $(2\pi/\sigma)(d\sigma_{00}/d\omega_t)$, which is corresponds to a simple differential cross-section (DCS), merely describes the scattering direction of the product. The scattering direction of the product NeH$^+$ is associated to the collision energies. From Fig. 6(a), the product NeH$^+$ is not only forward scattering but also backward scattering at E_{col}=20kcal/mol, and backward scattering is stronger than forward scattering. With the increase of collision energy from 20 to 60 kcal/mol, the tendency of forward scattering
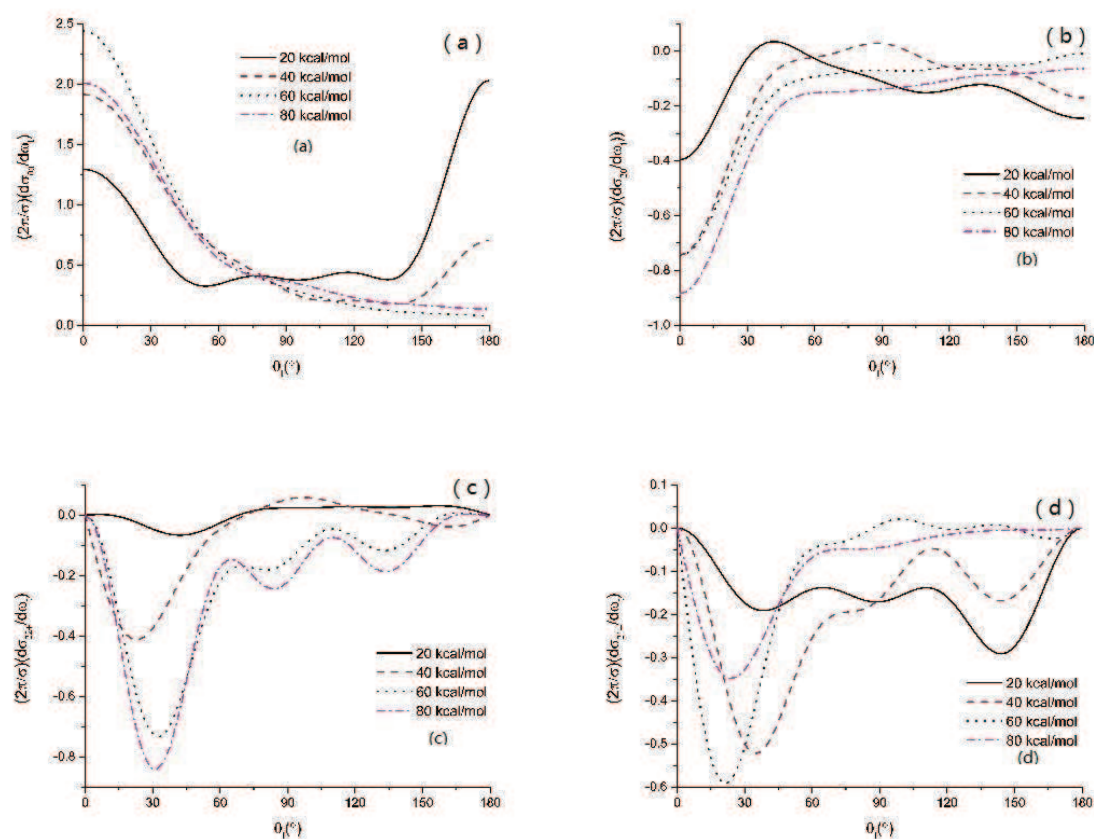
Figure 6: PDDCSs of NeH$^+$ from H + NeH$^+$ (v=0, j=0) $\rightarrow$ H + NeH$^+$ at E_{col}=20, 40, 60 and 80 kcal/mol.

increases and backward scattering decreases, however, it is opposite with the increased continuously of collision energy at above 60 kcal/mol. The PDDCS $(2\pi/\sigma)(d\sigma_{20}/d\omega_t)$ is related to the expectation value of the second Legendre moment $\langle P_2(\cos\theta_r)\rangle$. The trend of $(2\pi/\sigma)(d\sigma_{20}/d\omega_t)$ is basically opposite to that of $(2\pi/\sigma)(d\sigma_{00}/d\omega_t)$. As is shown in Fig. 6(b), j' is preferentially polarized along the direction perpendicular to k at θ_t=0°. As shown in Figs. 6(c) and 6(d), the $(2\pi/\sigma)(d\sigma_{22+}/d\omega_t)$ and $(2\pi/\sigma)(d\sigma_{21-}/d\omega_t)$ with $q\neq0$ are equal zero at the extremities of forward and backward scattering. At these limited scattering angles, the k-k' scattering plane is not determined and the value of these PDDCSs with $q\neq0$ must be zero [28]. The PDDCSs is related to $\langle\sin^2\theta_r\cos2\varphi_r\rangle$, and it is clear that the value of $(2\pi/\sigma)(d\sigma_{22+}/d\omega_t)$ is negative for most of all the scattering angles, which indicates the prominent preference of product alignment along the y-axis. It is interesting that four collision energies have a consistent polarization trend for $(2\pi/\sigma)(d\sigma_{22+}/d\omega_t)$. The strongest polarization of the product molecule is at about 30°, and the product shows a stronger polarization at E_{col}=60 kcal/mol. The value of $(2\pi/\sigma)(d\sigma_{21-}/d\omega_t)$ is relative to $\langle-\sin^2\theta_r\cos2\varphi_r\rangle$, and the behavior of it changes as

the collision energy increases. As is shown in Fig. 6(d), it is clear that the value of $(2\pi/\sigma)(d\sigma_{21-}/d\omega_t)$ is negative for most of all the scattering angles, which indicates the product alignment is along the direction of vector x+z.

4 Conclusions

In this paper, we use the quasi-classical trajectory method to research the vector correlations between the reagent and product for reaction H + NeH$^+$ (v=0, j=0) $\rightarrow$ H + NeH$^+$ at different collision energies. With the increasing collision energy, the integral cross-section of the title reaction decreases and then increases. For the reaction H + NeH$^+$ (v=0, j=0) $\rightarrow$ H + NeH$^+$, the influence of collision energy is studied and the distributions of $P(\theta_r)$, $P(\phi_r)$ and four PDDCSs are calculated. The results present that the rotational polarization of product NeH$^+$ has different characteristics at different collision energies. The products are mostly forward scattering at four collision energies, and the tendency of forward scattering increases quickly with the increasing of collision energy. The product rotational angular momentum vector j' is preferentially oriented along the positive direction of y-axis at low collision energy, and preferentially oriented along the negative direction of y-axis at high collision energy. In addition, the average rotational alignment parameter $P_2\langle(j\cdot k)\rangle$ of products is calculated, and the tendency of it agrees well with the distribution of $P(\theta_r)$.

References

[1] P. Pendergast, J. M. Heck, E. F. Hayes, R. Jaquet, J. Chem. Phys. 1993, 98, 4543.
[2] J. D. Kress, R. B. Walker, E. F. Hayes, P. Pendergast, J. Chem. Phys. 1994, 100, 2728.
[3] M. Gilibert, R. M. Blasco, M. González, X. Giménez, A. Aguilar, I. Last, M. Baer, J. Phys. Chem. A 1997, 101, 6821.
[4] M. Gilibert, X. Giménez, F. Huarte-Larrañaga, M. González, A. Aguilar, I. Last, M. Baer, J. Chem. Phys. 1999, 110, 6278.
[5] J. Mayneris, J. D. Sierra, M. González, J. Chem. Phys. 2008, 128, 194307.
[6] J. Mayneris-Perxachs, M. González, J. Phys. Chem. A 2009, 113, 4105.
[7] S.-J. Lv, P.-Y. Zhang, K.-L. Han, G.-Z. He, J. Chem. Phys. 2010, 132, 014303.
[8] J. Xiao, C.-L. Yang, M.-S. Wang, X.-G. Ma, Chin. Phys. Lett. 2011, 28, 013101.
[9] J. Xiao, C.-L. Yang, M.-S. Wang, X.-G. Ma, Chem. Phys. 2011, 379, 46.
[10] J. Xiao, C.-L. Yang, M.-S. Wang, Chin. Phys. B 2012, 21, 043101.
[11] Y. Wang, B. Tian, L. Qu, J. Chen, H. Li, Bull. Korean Chem. Soc. 2011, 32, 4210.
[12] M. H. G, Y. J. Zheng, Chin. Phys. B 2011, 20, 083401.

[13] J.-h. Zou, S.-H. Yin, M.-X. Guo, X.-S. Xu, L. Che, L. Li, H. Gao, Bull. Chem. Soc. Jpn. 2013, 86, 472.

[14] S.-H. Yin, J.-h. Zou, M.-X. Guo, L. Li, X.-S. Xu, H. Gao, L.Che, Chin. Phys. B, 2013, 22, 028201.

[15] S.-H. Yin, J.-h. Zou, M.-X. Guo, L. Li, X.-S. Xu, H. Gao, L.Che, Chin. Sci. Bull, 2012, 57,4712.

[16] E. R. Davidson, D. W. Silver, Chem. Phys. Lett, 1977, 52, 403.

[17] A. Aguado, M. Paniagua, J. Chem. Phys, 1992, 96, 1265.

[18] T. Zhang, X.-M. Qian, X.-N. Tang, J. Chem.Phys, 2003, 119, 10175.

[19] S.-H. Yin, J.-h. Zou, M.-X. Guo, L. Li, X.-S. Xu, H. Gao, L. Che, Int J. Quant. Chem, 2011, 111, 4400.

[20] S.-H. Yin, J.-h. Zou, M.-X. Guo, L. Li, X.-S. Xu, H. Gao, L. Che, Comput. Theor. Chem, 2011, 967, 19.

[21] F. J.Aoiz, M. Brouard, P.A.Enriquez, J. Chem. Phys, 1996, 105, 4964.

[22] M. Brouard, H. M. Lambert, S. P. Rayner, Mol. Phys, 1996, 89, 403.

[23] H. Häkkinen, M. Moseler, U. Landman, Phys. Rev. Lett.89 (2002) 033401.

[24] C.-H. Zhang, W.-Q Zhang, M.-D. Chen, J.Theor. Comput. Chem, 2009, 8, 403.

[25] W.-Q. Zhang, M.-D. Chen, J. Theor. Comput. Chem, 2009, 8, 1131.

[26] R.-J. Li, K.-L. Han, F.-E. Li, Chem. Phys. Lett, 1994, 220, 281.

[27] K.-L. Han, L. Zhang, D.-L. Xu, J. Phys. Chem. A, 2001, 105, 2956.

[28] S. Gómez-Carrasco, M. L. Hernándezb. Chem. Phys. Lett, 2007, 435,188.